

Finding rational regimes for direct fabrication of long products from powders of refractory compounds by SHS extrusion

© Lyubov' S. Stel'makh^a, Alexandra O. Zhidovich^a✉, Alexander M. Stolin^a, Sergey V. Karpov^b

^a *Merzhanov Institute of Structural Macrokinetics and Materials Science RAS (ISMAN),
8, Academician Osipyan St., Chernogolovka, 142432, Russian Federation,*

^b *Tambov State Technical University, Bld. 2, 106/5, Sovietskaya St., Tambov, 392000, Russian Federation*

✉ a10012012*@ism.ac.ru

Abstract: For qualitative and quantitative analysis of self-propagating high-temperature synthesis (SHS) in combination with SHS extrusion, thermal and rheodynamic models, which use data on the actual conditions of the technological process, were developed. In this paper, to assess the effect of technological and thermal parameters on the length of extruded rods, mathematical modeling of the process of SHS extrusion of a material based on titanium diboride with the initial molar composition Ti-2B-0.9Co was carried out. The real combustion temperatures of the system, obtained experimentally under various conditions (relative density, grade of titanium powder), were used in the model calculations. On the basis of mathematical models of the thermal regimes of SHS processes, the temperature fields in the sample material in a cylindrical mold, in a heat insulator, and also in an extruded rod were studied, and the lengths of the resulting rods were determined depending on various technological parameters of the process. Rods were obtained experimentally by SHS extrusion, confirming the correctness of the numerical results of the prediction based on mathematical modeling. Theoretical studies of the SHS extrusion process, based on the effect of high-temperature shear deformation on synthesis products in a hot state, contribute to the development and creation of new advanced SHS technological methods for producing composite and cermet materials and products.

Keywords: SHS extrusion; metal-ceramic materials; electrodes for surfacing; mathematical model; simulation of thermal regimes.

For citation: Stel'makh LS, Zhidovich AO, Stolin AM, Karpov SV. Finding rational regimes for direct fabrication of long products from powders of refractory compounds by SHS extrusion. *Journal of Advanced Materials and Technologies.* 2022;7(3):172-180. DOI:10.17277/jamt.2022.03.pp.172-180

Установление рациональных режимов прямого получения длинномерных изделий из порошков тугоплавких соединений методом СВС-экструзии

© Л. С. Стельмах^a, А. О. Жидович^a✉, А. М. Столин^a, С. В. Карпов^b

^a *Институт структурной макрокинетики и проблем материаловедения
им. А. Г. Мерджанова Российской академии наук (ИСМАН),
ул. Академика Осипьяна, д. 8, Черноголовка, Московская область, 142432, Российская Федерация,*

^b *Тамбовский государственный технический университет,
ул. Советская, 106/5, пом. 2, Тамбов, 392000, Российская Федерация*

✉ a10012012@ism.ac.ru

Аннотация: Для качественного и количественного анализа самораспространяющегося высокотемпературного синтеза в сочетании с экструзией (СВС-экструзия) разработаны тепловые и реодинамические модели, в которых используются данные о реальных условиях протекания технологического процесса. В данной работе для оценки влияния технологических и тепловых параметров на длину экструдированных стержней проведено математическое моделирование процесса СВС-экструзии материала на основе диборида титана исходного

мольного состава Ti–2B–0,9Co. В расчетах модели использовались реальные температуры горения системы, полученные экспериментально при различных условиях (относительная плотность, марка порошка титана). На основе математических моделей тепловых режимов СВС-процессов исследованы температурные поля в материале образца, находящегося в цилиндрической пресс-форме, в теплоизоляторе, а также в экструдированном стержне, определены длины получаемых стержней в зависимости от различных технологических параметров процесса. Экспериментально методом СВС-экструзии получены стержни, подтверждающие правильность численных результатов прогноза на основе математического моделирования. Теоретические исследования процесса СВС-экструзии, основанного на воздействии высокотемпературного сдвигового деформирования на продукты синтеза, находящиеся в горячем состоянии, способствуют развитию и созданию новых передовых технологических методов СВС для получения композиционных и металлокерамических материалов и изделий.

Ключевые слова: СВС-экструзия; металлокерамические материалы; электроды для наплавки; математическая модель; моделирование тепловых режимов.

Для цитирования: Stel'makh LS, Zhidovich AO, Stolin AM, Karpov SV. Finding rational regimes for direct fabrication of long products from powders of refractory compounds by SHS extrusion. *Journal of Advanced Materials and Technologies. 2022;7(3):172-180. DOI:10.17277/jamt.2022.03.pp.172-180*

1. Introduction

An important issue of developing the SHS technology [1–4] was to study the possibility of direct fabrication of products of the desired shape, size, composition, structure, and, ultimately, with desired performance properties, bypassing the stage of preparing powders of the final product. When using the combined action of shear deformation and pressure in the process of SHS extrusion, new possibilities open up for one-stage fabrication of products from powders of refractory compounds.

The combination of combustion processes and high-temperature shear deformation makes it possible to use the internal energy of the reacting system released during the chemical reaction, and thereby avoid the need for external heating and long-term exposure. This provides the appearance of new features in the process of structure formation of materials [5, 14]. Note that this method is science-intensive and opens up a fundamentally new approach to the organization of the technological process of manufacturing long products from brittle and hard-to-deform powders of refractory inorganic compounds in the cold state.

Previously, to study the abrupt cooling of SHS synthesis products, thermal models were formulated that describe non-stationary thermal processes in combustion products and their heat exchange with the environment under real conditions of SHS extrusion [15, 16].

The development of affordable and economical methods for preparing coatings on the surface of a tool and process equipment based on cermet composite materials (CCMs) based on titanium alloys is a promising direction. Titanium borides are effective hardeners, since it has a high Young's modulus, high strength, and a similar thermal

expansion coefficient. In addition, they are chemically inert with respect to the matrix of the metal binder [17–19]. In turn, titanium borides are characterized by high hardness, wear resistance, heat resistance, and heat resistance [20–24]. In this regard, it can be concluded that materials with a complex structure of titanium monoboride, titanium diboride and a metal binder, in various mass ratios, should be used in hard, heat-resistant and wear-resistant coatings for products for a wide range of purposes [23–28]. Such composites combine the plasticity and toughness of a titanium matrix with high strength, hardness, rigidity, and heat resistance.

In this paper, using mathematical modeling of the thermal regimes of SHS extrusion [15, 16], we studied the effect of processing and thermal parameters on the length of electrodes for surfacing from a cermet material based on titanium diboride with additionally introduced cobalt.

2. Materials and Methods

2.1. Object of study

For experimental studies, charge blanks, or tablets with a diameter of 25 mm, were prepared by direct pressing. The molar ratios of the initial components were Ti : B : Co = 1 : 2 : 0.9, the relative density was 0.55–0.70. Titanium powders of different granulometric composition were used. The particle size of the main fraction was: 65–150 microns for titanium powder No. 1; 15–25 microns for #2 and 100–170 microns for #3.

In the Ti–B–Co system under study, the synthesis of the material in the combustion mode is ensured due to the high exothermicity of the chemical reaction of the interaction of titanium and boron powders with the formation of titanium diboride and boride, respectively: $Ti + 2B \rightarrow TiB_2$.

2.2. Numerical method

Previously developed mathematical models of the thermal regimes of the SHS extrusion process [15, 16] make it possible to study the temperature fields in the sample material located in a cylindrical mold, a heat insulator, and an extruded rod depending on various process parameters (combustion temperature, delay time, plunger speed press, heating temperatures of various equipment zones, etc.). The length of the extruded rod was predicted. When a part of the material located in the profiling matrix and located directly above its hole lost its “survivability” (the temperature became lower than the survivability temperature), i.e. the ability to plastic deformation, and clogged the outlet, the extrusion stopped. The resulting length – the ordinate of the lower boundary of the sample – was the desired length of the product.

For this purpose, the system of differential equations [15] for a heat insulator (asbestos):

$$\frac{\partial T_1}{\partial t} = a_1 \nabla^2 T_1 = a_1 \left(\frac{\partial^2 T_1}{\partial r^2} + \frac{1}{r} \frac{\partial T_1}{\partial r} + \frac{\partial^2 T_1}{\partial z^2} \right) \quad (1)$$

and the sample material in the mold and extruded rod was numerically studied:

$$c \left(\frac{\partial(\rho T_2)}{\partial t} + f(\rho, z) \frac{\partial T_2}{\partial z} \right) = \lambda_2(\rho) \nabla^2 T_2. \quad (2)$$

Depending on the stage of the process, the functions $f(\rho, z)$ and $\lambda_2(\rho)$ included in the differential equations have the following values:

$$f(\rho, z) = \begin{cases} 0 & \text{(I)} \\ \rho U_n z & \text{(II)} \\ \frac{H_0}{Q} & \text{(III)} \\ \frac{Q}{\pi R^2(z)} & \text{(III)} \end{cases}$$

$$\lambda_2(\rho) = \begin{cases} \lambda_0 \text{(I)} \\ \lambda_0 \left(\frac{\rho_0(1 - U_n t / H_0)}{\rho_0} \right)^k & \text{(II)}, \\ \lambda_k \text{(III)} \end{cases}$$

where I, II, and III are stages of combustion-delay, pressing and extrusion (extrusion), respectively. As a result of the numerical solution of a two-dimensional thermal problem with two moving boundaries, the temperature field $T = T(r, z, t)$ was found, which is a function of two coordinates r and z and time t in the sample, heat insulator, extruded

(extruded) part of the material, and the length of the product was predicted (L). Differential equations, initial and boundary conditions were reduced to a dimensionless form. The problem was solved by the finite difference method using a four-point difference scheme. Each of equations (1) and (2) is split into two and presented in finite difference form. The obtained difference equations were solved by the sweep method in single-layer regions and by the through-sweep method in two-layer regions.

As a result of a numerical study, graphs of the temperature fields in the sample, heat insulator and extruded rod, as well as its length, are displayed.

Note that for each specific practical application, it is necessary to solve problems directly related to the manufacturing technology of the considered products and the technical characteristics of these products. Experimental research causes difficulties, and methods of mathematical modeling make it possible to investigate an object by simulating an experiment on a computer and thus exclude or significantly reduce the volume of the experiment. It should be emphasized the predominant applied nature of these studies, which are characterized by a comprehensive implementation of its results in the practice of solving specific technological problems.

The main task of theoretical consideration for thermal and rheodynamic models of SHS extrusion is the analysis of the density, temperature, and stress-strain state of the material depending on pressure, as well as on the initial distribution of temperature and density over the sample volume. An essential side of this line of research is the use of specific data on the actual conditions of the technological process, which in conventional theoretical studies of SHS processes were given in the most general form. In this study, at the preliminary stage, the combustion temperatures of the studied composition were experimentally determined under various conditions (relative density of blanks, powder grades).

The following data were used in the calculations for the material of the initial molar composition Ti-2B-0.9Co: pressure on the press plunger $P = 10^8$ Pa, density of the incompressible base of the material $\rho_1 = 5.58 \times 10^3$ kg·m⁻³, initial sample density $\rho_0 = 3.13 \times 10^3 - 3.99 \times 10^3$ kg·m⁻³, heat capacity $c = 1750 - 1759$ J·(kg·K)⁻¹, coefficient of thermal conductivity of the composition $\lambda = 18 - 46$ W·(m·K)⁻¹, initial sample height $H_0 = 40 \times 10^{-3}$ m, billet diameter $d_1 = 25 \times 10^{-3}$ m, combustion temperature $T_c = 2269 - 2395$ K, molding temperature $T_1 = 1087 - 1398$ K ($T_1 = (0.7 - 0.9)T_{\text{melt}}$, where melting temperature of the

binder $T_{\text{melt}} = 1553$ K), composition burning rate $U_c = 300 \times 10^{-3} - 375 \times 10^{-3} \text{ m} \cdot \text{s}^{-1}$, press plunger speed $U_n = 61 \times 10^{-3} \text{ m} \cdot \text{s}^{-1}$, die cone angle $2\alpha = 180^\circ$, profiling matrix hole diameter $d_3 = 3 \times 10^{-3} - 5 \times 10^{-3} \text{ m}$, gauge diameter $d_2 = 3 \times 10^{-3} - 5 \times 10^{-3} \text{ m}$, asbestos thickness on the matrix and in the hole $\delta = 1.5 \times 10^{-3} \text{ m}$.

2.3. Experimental methods

The combustion temperature of the SHS process was determined by the thermocouple method on a TEST model facility developed at the ISMAN Laboratory for Plastic Deformation of Materials. The installation allows to carry out studies under the conditions in which the sample is located during synthesis in an extrusion mold, including under the same heat transfer conditions. Two holes for thermocouples were drilled in charge blanks thermally insulated with asbestos cloth (thickness 1.5 mm) at a known distance l to a depth of 12.5 mm. Then the samples were placed in a cylindrical chamber with dimensions corresponding to the dimensions of a real extrusion mold, and thermocouples were fed through special holes in the chamber. The SHS process was initiated from the uninsulated end of the tablet using a tungsten coil. As a result, the combustion temperature profiles were obtained, which were used to determine the maximum temperature realized in the SHS process (it is also the combustion temperature), and also the charge combustion rate was calculated using the formula:

$$V_c = \frac{l}{\tau_2 - \tau_1},$$

where l is distance between thermocouples, mm; τ_2 is point in time at which the maximum temperature value is read from thermocouple 2, s; τ_1 is point in time at which the maximum temperature value is read from thermocouple 1, s.

Rods from the material of the initial molar composition Ti-2B-0.9Co were obtained by SHS extrusion (Fig. 1). The charge billet was placed in a special extrusion mold, the combustion process was initiated using a tungsten spiral, and after the combustion wave passed through the entire sample, after a certain time (delay time), under the influence of pressure P , the synthesized cermet material was pressed through the forming matrix. A detailed description of the SHS extrusion process can be found in [5, 14].

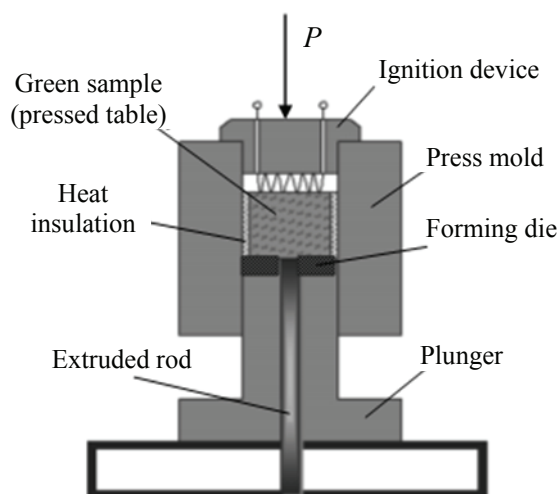


Fig. 1. Schematic view of the installation for SHS extrusion

3. Results and Discussion

3.1. Results of numerical studies of the Ti-B-Co system

Temperature distribution at different stages of the SHS extrusion process and the correlation between the rod length and the hole diameter of the profiling die. Figure 2 shows the temperature fields of the extruded material at three stages of the SHS extrusion process: a) combustion stage, b) pressing stage, c) extrusion stage. Since the sample is located in a cold mold, the temperature near its walls is somewhat lower than in the middle of the sample. At the stage of extrusion, when the synthesized material passes through a cold forming matrix, it is additionally cooled to 0.75–0.80 of the temperature of the middle of the sample, close to the combustion temperature during the SHS process. The temperature of the formed rod at the exit from the matrix is 0.30–0.35 of the temperature of the material after the synthesis reaction. When the synthesized material cools to temperatures below the pot life temperature, the material loses its ability to form, as a result, the outlet of the profiling matrix is clogged and the extrusion process stops.

The dependence of the rod length on the radius of the hole – the radius of the resulting rod is shown in Fig. 3. For the synthesized material based on titanium diboride, the length of the rods decreases with an increase in their diameter. The dependence obtained as a result of the numerical study corresponded to the experimental data.

The correlation between the rod length and the initial porosity (density) of the sample. The length of the rods produced by SHS extrusion from the Ti-2B-0.9Co material was studied numerically.

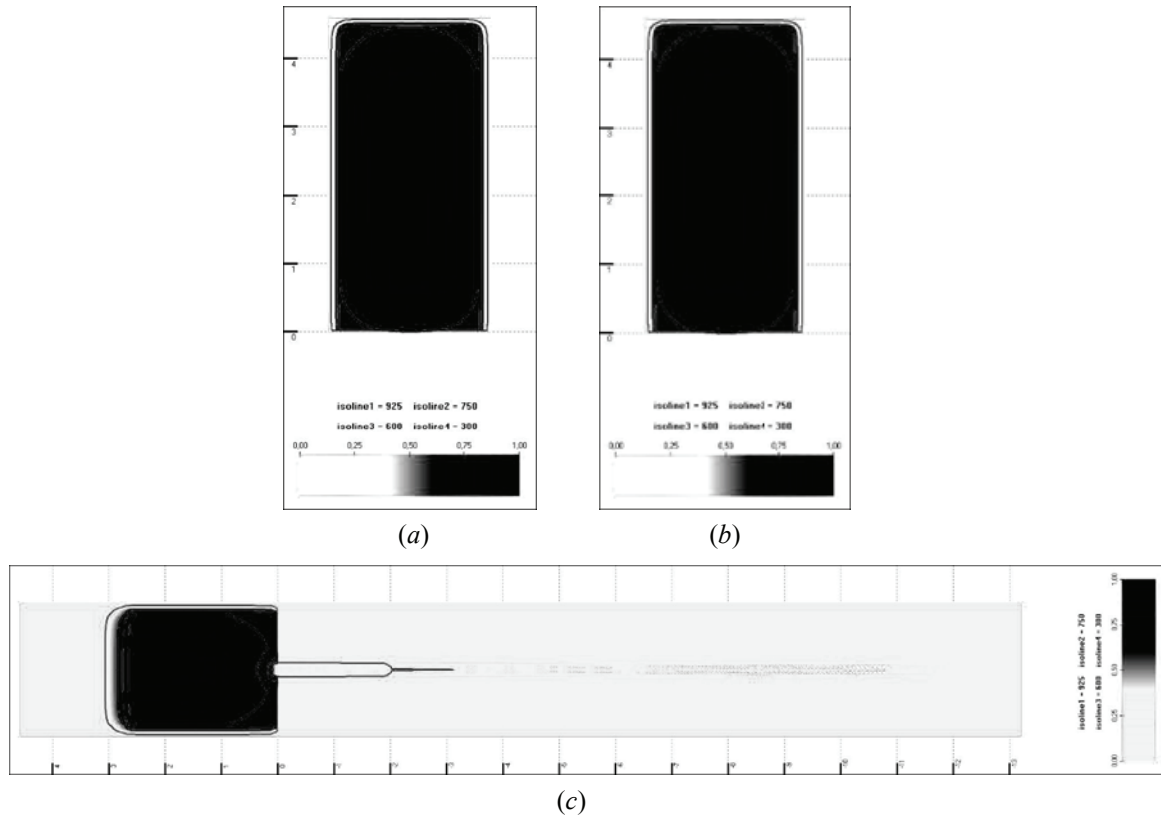


Fig. 2. Temperature distribution in the sample at the stages of: *a* – combustion-delay; *b* – pressing; *c* – extrusion. Parameters: hole radius of the profiling matrix $r_1 = 1.5$ mm (rod diameter $d_1 = 3$ mm), matrix angle 180 degrees, press plunger speed $V = 61 \text{ mm}\cdot\text{s}^{-1}$, asbestos thickness around the sample $Asb = 1.5$ mm. The initial height of the tablet $H_0 = 40$ mm, the length of the extruded part $L = 162$ mm

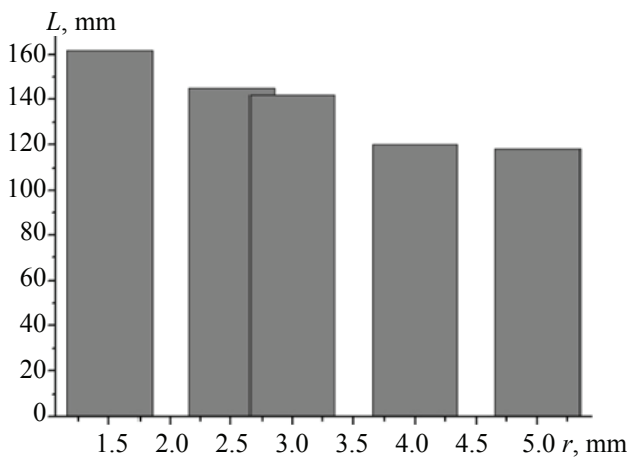


Fig. 3. The correlation the length of the extruded rod (L) and the hole radius of the profiling matrix (r). Parameters: die angle 180 degrees, press plunger speed $V = 61 \text{ mm}\cdot\text{s}^{-1}$, asbestos thickness around the sample $Asb = 1.5$ mm, sample initial height $H_0 = 40$ mm, the degree of deformation is constant

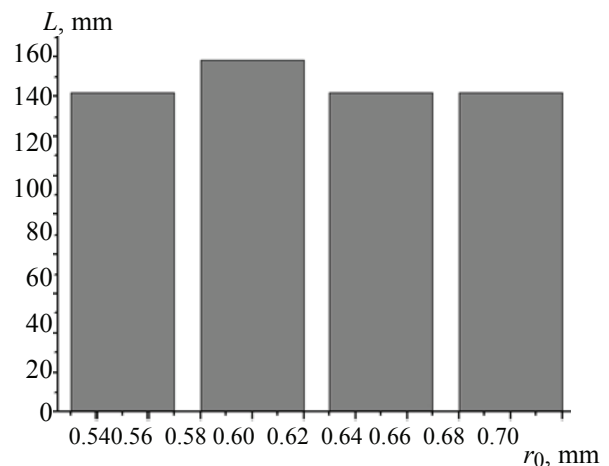


Fig. 4. The correlation between the length of the extruded rod (L) and the initial density (r_0). Parameters: die angle 180 degrees, press plunger speed $V = 61 \text{ mm}\cdot\text{s}^{-1}$, asbestos thickness around the sample $Asb = 1.5$ mm, sample initial height $H_0 = 40$ mm, rod radius $R_0 = 2.5$ mm, $\rho_0 = 0.5\text{--}0.7$, the degree of deformation is constant

The initial density of powder blanks affects the combustion temperature of the material. In this regard, the processing interval of the material also changes. Figure 4 shows the dependence of the length

of the rod on the initial density. It can be seen that it is nonmonotonic and has a maximum at a relative density of 0.6; the length of the extruded rods under such conditions was 178 mm.

The correlation between the rod length and the delay time and temperature of material survivability. An important parameter of SHS extrusion is the pressure delay time. The moment when the combustion front has passed through the entire sample is taken as the beginning of the countdown of the delay time, that is, the synthesis of the material has taken place in the entire volume of the sample. As numerical calculations show (Fig. 5), a decrease in this time leads to an increase in the length of the extruded part of the rod from 162 to 194 mm (by 20 %), for a rod radius of 1.5 mm. This is due to the fact that at a higher temperature the material has a greater ability to deform (plasticity).

An important parameter is the molding temperature (survivability) for predicting the length of the resulting rods. It is usually in the range of 0.7–0.9 of the melting point of the binder. It is desirable to measure it in an experiment in order to obtain more accurate predictions from a mathematical model. Figure 6 shows the dependences of the length of the rods on the survivability temperature for the pressure supply delay times of 0, 2, and 4.3 s.

It can be seen that the length of the resulting rods can reach values of more than 300 mm under extrusion conditions immediately after the combustion wave has passed through the entire sample or with a delay time of 0 s. It should also be noted that an increase in the time and interval of survivability, and hence the length of the rods, is ensured when the synthesized material has the necessary plasticity for its extrusion at relatively low temperatures (1100 K).

The correlation between the particle size distribution of titanium powder and the length of the resulting rods. The length of the rods produced by SHS extrusion from powder mixtures of the Ti–B–Co

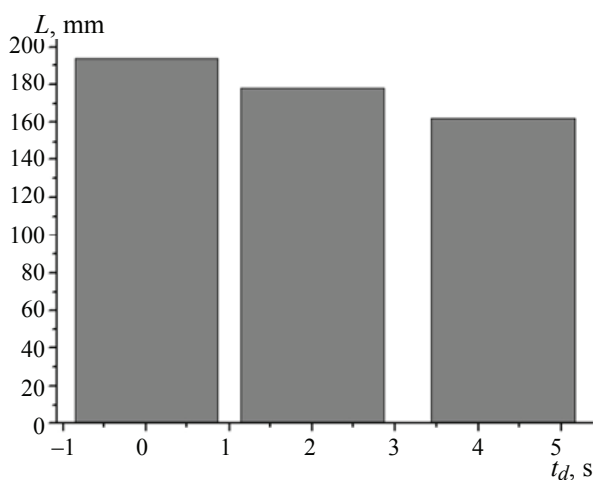


Fig. 5. Influence of the delay time (t_d) on the rod length (L). Parameters: $r_1 = 1.5$ mm, $V = 61$ mm·s⁻¹, $H_0 = 40$ mm

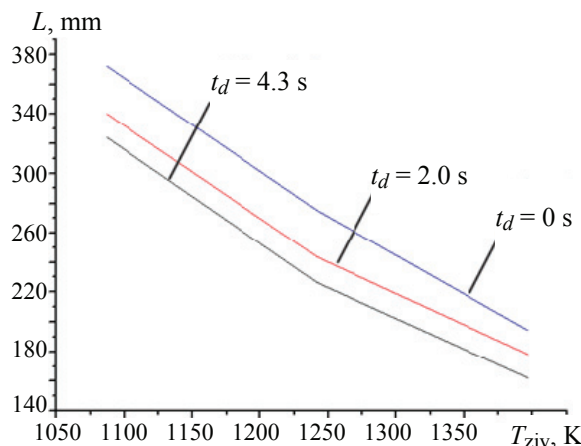


Fig. 6. The correlation between the length of the extruded rod (L) and the temperature of survivability (T_j) for different delay times: black line – 4.3 s, red – 2 s, blue – 0 s. Parameters: die angle 180 degrees, press plunger speed $V = 61$ mm·s⁻¹, asbestos thickness around the sample $Asb = 1.5$ mm, sample initial height $H_0 = 40$ mm, rod radius $R_0 = 2.5$ mm, the degree of deformation is constant

system was numerically studied depending on the brand of titanium powders used (No. 1: the main weight fraction of particles is in the range of 65–150 microns; No. 2: 15–25 microns; No. 3: 100–170 microns). According to experimental data, the mixture with titanium powder No. 3 has the highest combustion temperature of 2341 K (Fig. 7). For mixtures with titanium No. 1 and No. 2, the combustion temperature was 2313 K and 2219 K, respectively.

From the results of numerical studies (Fig. 8) it can be seen that for a relative initial density of 0.6–0.7, a powder with a particle size of 100–170 microns (No. 3) is preferable. The length of the rods when using these powders is 1.12 times greater. With the improvement of the thermal conditions of the process (heating of the tablet, thermal insulation), the length can be increased.

3.2. Results of experiments performed on the basis of the constructed mathematical models for the Ti–B–Co system

Based on the results of mathematical modeling, experiments were carried out to obtain rods from the studied material Ti–2B–0.9Co by SHS extrusion with different delay times at an optimal relative density of 0.6 (Fig. 9). The lifetime temperature of the extruded material, based on the experiments, was $T_{ziv} = 1350$ –1400 K. When comparing the theoretical data with the experimental data, it can be seen that for a delay

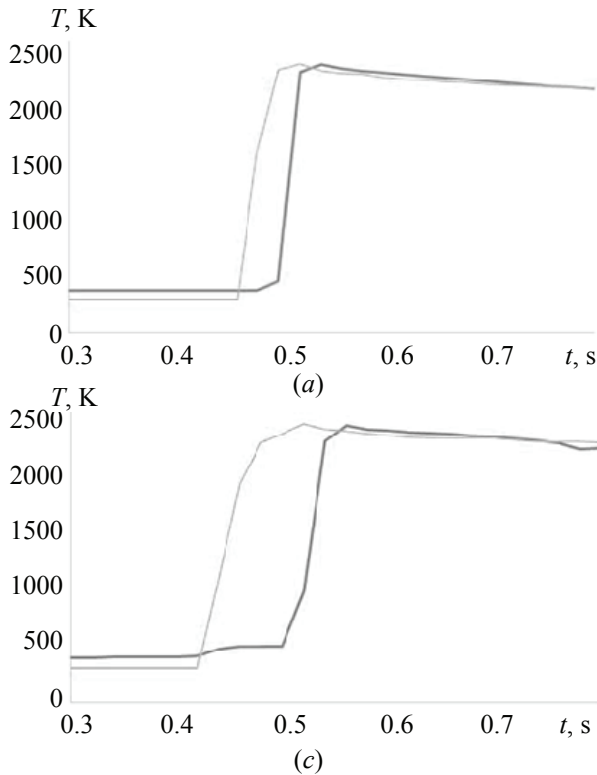


Fig. 7. Temperature profiles of combustion of a mixture of powders of the Ti– B–Co system with the initial component of titanium powder No. 1 (a), No. 2 (b), No. 3 (c)

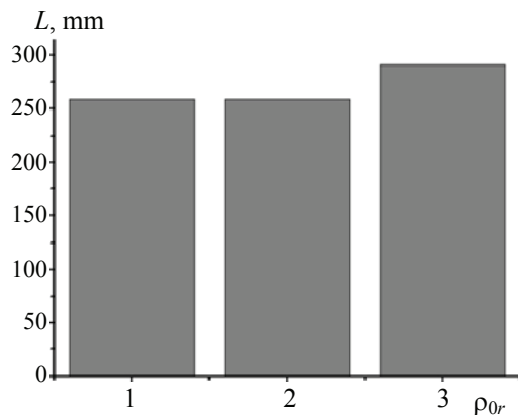


Fig. 8. Correlation between the length of the extruded rod (L) and the particle size distribution of the titanium powder used: No. 1, No. 2, No. 3. Parameters: die angle 180 degrees, press plunger speed $V = 61 \text{ mm}\cdot\text{s}^{-1}$, asbestos thickness around the sample $Asb = 1.5 \text{ mm}$, sample initial height $H_0 = 40 \text{ mm}$, rod radius $R_0 = 2.5 \text{ mm}$, constant deformation degree

time of about 4.3 s, the numerical calculations of the rod length using the mathematical model are in good agreement with practical data. With an increase in the delay time to 4.6 s, the plasticity of the material decreases, and the length of the extruded rod decreases by about 4 times. With a delay time of 5.0 s or more, heat losses lead to a critical decrease in the rheological properties of the material, at which it is not possible to extrude it.

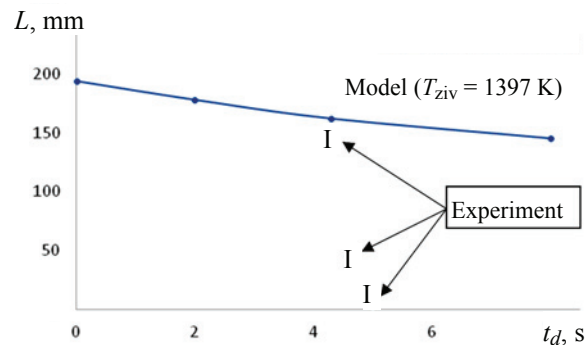


Fig. 9. Correlation between the rod length and the delay. Parameters: die angle 180 degrees, press plunger speed $V = 61 \text{ mm}\cdot\text{s}^{-1}$, asbestos thickness around the sample $Asb = 1.5 \text{ mm}$, sample initial height $H_0 = 40 \text{ mm}$, rod radius $R_0 = 1.5 \text{ mm}$, deformation degree is constant

4. Conclusions

The temperature fields in the sample material were studied using the developed mathematical models of the thermal regimes of SHS extrusion. It was found that the temperature of the synthesized material Ti–2B–0.9Co while pressing through the forming die was higher than the survivability temperature, which makes it possible to produce rods with a length of more than 100 mm. It is proved that an increase in the hole radius of the profiling matrix from 1.5 mm to 5 mm leads to a reduction in the length of the rod by 25 %.

It was found that for the Ti–2B–0.9Co material, the dependence of the length of the extruded rod on

the initial porosity (density) is extreme and has a maximum (178 mm) at a relative density of the initial billet equal to 0.6.

It is shown that a decrease in the temperature of the survivability of the synthesized material leads to a decrease in the length of the extruded rod, since the temperature-time interval in which the material has sufficient plasticity for its extrusion decreases.

Both numerical and experimental studies of the influence of the delay time on the length of an extruded rod made of Ti–2B–0.9Co material showed that with an increase in the delay time, the ability of the material to extrude decreases. When extrusion was carried out 4.3 s after SHS of the material in the entire volume of the sample, the difference between the theoretically calculated and experimentally obtained length of the rods was 7.5 %.

It was found that the use of titanium powder in the initial mixtures with the main weight fraction of large particles 100–170 μm in size makes it possible to increase the length of the rods obtained by SHS extrusion by 1.12 times compared to titanium powders, the size of the main weight fraction of particles of which has a spread of 15–25 and 65–150 microns.

The presented theoretical and experimental studies will be continued due to their great practical importance in choosing the optimal parameters of SHS extrusion for the development of an experimental batch of surfacing electrodes in order to apply protective coatings on the bits of agricultural machines (work is carried out jointly with Tambov State Technical University).

5. Funding

This study did not receive external funding.

6. Conflict of interests

The authors declare no conflict of interest.

References

1. Merzhanov AG. SHS technology. *Advanced Materials*. 1992;4(4):294-295. DOI:10.1002/adma.19920040412
2. Levashov EA, Mukasyan AS, Rogachev AS, Shtansky DV. Self-propagating high-temperature synthesis of advanced materials and coatings. *International Materials Reviews*. 2017;62(4):203-239. DOI:10.1080/09506608.2016.1243291
3. Liu G, Chen K, Li J. Combustion synthesis: an effective tool for preparing inorganic materials. *Scripta Materialia*. 2018;157:167-173. DOI:10.1016/j.scriptamat.2018.08.022
4. Liu G, Li J, Chen K. Combustion synthesis of refractory and hard materials: A review. *International Journal of Refractory Metals and Hard Materials*. 2012;39:90-102. DOI:10.1016/j.ijrmhm.2012.09.002
5. Stolin AM, Bazhin PM. Manufacture of multipurpose composite and ceramic materials in the combustion regime and high-temperature deformation (SHS extrusion). *Theoretical Foundations of Chemical Engineering*. 2014;48(6):751-763. DOI:10.1134/S0040579514060104
6. Cheng T, McLean M. Hot extrusion reaction synthesis: simultaneous synthesis and forming from element powders. *Materials Letters*. 1996;29:91-99. DOI:10.1016/S0167-577X(96)00124-3
7. Morsi K, McShane HB, McLean M. Processing defects in hot extrusion reaction synthesis. *Materials Science and Engineering A*. 2000;290(1):39-45. DOI:10.1016/S0921-5093(00)00932-1
8. Gao T, Liu LY, Song JP, Liu GL, Liu XF. Synthesis and characterization of an in-situ Al₂O₃/Al–Cu composite with a heterogeneous structure. *Journal of Alloys and Compounds*. 2021;868:159283. DOI:10.1016/j.jallcom.2021.159283
9. Morsi K, Moussa SO, Wall JJ. Simultaneous combustion synthesis (thermal explosion mode) and extrusion of nickel aluminides. *Journal of Materials Science*. 2005;40(4):1027-1030. DOI:10.1007/s10853-005-6526-z
10. Minay EJ, McShane HB, Rawlings RD. The hot extrusion reaction synthesis of nickel aluminide alloys. *Intermetallics*. 2004;12:75-84. DOI:10.1016/j.intermet.2003.09.009
11. Vallauri D, Shcherbakov VA, Khitev AV, Deorsola FA. Study of structure formation in TiC–TiB₂–Me_xO_y ceramics fabricated by SHS and densification. *Acta Materialia*. 2008;56(6):1380-1389. DOI:10.1016/j.actamat.2007.11.022
12. Dargar SR, Groven LJ, Swiatkiewicz JJ, Puszynski JA. In situ densification of SHS composites from nanoreactants. *International Journal of Self-Propagating High-Temperature Synthesis*. 2007;16:125-132. DOI:10.3103/S1061386207030041
13. Zhang X, He X, Han J, Qu W, Kvalin VL. Combustion synthesis and densification of large-scale TiC–xNi cermets. *Materials Letters*. 2002;56(3):183-187. DOI:10.1016/S0167-577X(02)00437-8
14. Bazhin PM, Stolin AM, Alymov MI. Preparation of nanostructured composite ceramic materials and products under conditions of a combination of combustion and high-temperature deformation (SHS extrusion). *Nanotechnologies in Russia*. 2014;9:583-600. DOI:10.1134/S1995078014060020
15. Stolin AM, Stel'makh LS. Mathematical modeling of SHS compaction/extrusion: An autoreview. *International Journal of Self-Propagating High-Temperature Synthesis*. 2008;17(2):93-100. DOI:10.3103/S1061386208020015
16. Parshin DA, Stelmakh LS, Stolin AM. SHS extrusion of thick rods: A numerical simulation. *International Journal of Self-Propagating High-Temperature Synthesis*. 2014;23(2):74-77. DOI:10.3103/S1061386214020071
17. Tjong, SC, Mai YW. Processing-structure-property aspects of particulate- and whisker reinforced titanium matrix composites. *Composites Science and Technology*. 2008;68:583-601. DOI:10.1016/j.compscitech.2007.07.016

18. Zhu YS, Liu YF, Wei XN, Sun D, Lu WZh, Ko TJ. Tribological characteristics of the dual titanium boride layers (TiB₂+TiB) on titanium alloy. *Ceramics International*. 2021;47(10):13957-13969. DOI:10.1016/j.ceramint.2021.01.265
19. Huang L, Qian M, Liu Z. In situ preparation of TiB nanowires for high-performance Ti metal matrix nanocomposites. *Journal of Alloys and Compounds*. 2018;735:2640-2645. DOI:10.1016/j.jallcom.2017.11.238
20. Ding HY, Zhou GH, Liu T, Xia MJ, Wang XM. Biotribological properties of Ti/TiB₂ multilayers in simulated body solution. *Tribology International*. 2015;89:62-66. DOI:10.1016/j.triboint.2015.02.004
21. Fattahi M, Ershadi MN, Vajdi M, Moghanlou FS, Namini AS, Asl MS. On the simulation of spark plasma sintered TiB₂ ultra high temperature ceramics: A numerical approach. *Ceramics International*. 2020;46(10):14787-14795. DOI:10.1016/j.ceramint.2020.03.003
22. Ravnikar D, Trdan U, Nagode A, Sturm R. Energy density effect of laser alloyed TiB₂/TiC/Al composite coatings on LMZ/HAZ, mechanical and corrosion properties. *Metals*. 2020;10(3):411-415. DOI:10.3390/met10030411
23. Kumar PS, Krishna VM, Kavimani V, Prakash KS, Kumar GS. Effect of TiB₂ on the corrosion resistance behavior of in situ al composites. *International Journal of Metalcasting*. 2020;14(1):84-91. DOI:10.1007/s40962-019-00330-3
24. Atturan UA, Nandam SH, Murty BS, Sankaran S. Deformation behaviour of in situ TiB₂ reinforced A357 aluminium alloy composite foams under compressive and impact loading. *Materials Science and Engineering A-Structural Materials Properties Microstructure and Processing*. 2017;684:178-185 DOI:10.1016/j.msea.2016.12.048
25. Zhang LC, Attar H. Selective laser melting of titanium alloys and titanium matrix composites for biomedical applications: A Review. *Advanced Engineering Materials*. 2016;18(4):463-475. DOI:10.1002/adem.201500419
26. Hao YL, Li SJ, Yang R. Biomedical titanium alloys and their additive manufacturing. *Rare Metals*. 2016;35(9):661-671. DOI:10.1007/s12598-016-0793-5
27. Zhou MY, Ren LB, Fan LL, Zhang YWX, Lu TH, Quan GF, Gupta M. Progress in research on hybrid metal matrix composites. *Journal of Alloys and Compounds*. 2020;838:155274. DOI:10.1016/j.jallcom.2020.155274
28. Bao Y, Huang LJ, An Q, Jiang S, Zhang R, Geng L, Ma XX. Insights into arc-assisted self-propagating high temperature synthesis of TiB₂-TiC ceramic coating via wire-arc deposition. *Journal of the European Ceramic Society*. 2020;40(13):4381-4395. DOI:10.1016/j.jeurceramsoc.2020.05.005

Information about the authors / Информация об авторах

Lyubov' S. Stel'makh, D. Sc. (Eng.), Leading Researcher, Merzhanov Institute of Structural Macrokinetics and Materials Science RAS (ISMAN), Chernogolovka, Russian Federation; ORCID 0000-0003-0418-1534; e-mail: stelm@ism.ac.ru

Alexandra O. Zhidovich, Junior Researcher, Merzhanov Institute of Structural Macrokinetics and Materials Science RAS (ISMAN), Chernogolovka, Russian Federation; ORCID 0000-0001-5083-1126; e-mail: a10012012@ism.ac.ru

Alexander M. Stolin, D. Sc. (Phys. and Math.), Professor, Head of the Laboratory, Merzhanov Institute of Structural Macrokinetics and Materials Science RAS (ISMAN), Chernogolovka, Russian Federation; ORCID 0000-0002-5360-3388; e-mail: amstolin@ism.ac.ru

Sergey V. Karpov, Cand. Sc. (Eng.), Associate Professor, chair "Computer-integrated systems in engineering", Tambov State Technical University, Tambov, Russian Federation; ORCID 0000-0001-8238-1537; e-mail: karpov.sv@mail.tstu.ru

Стедьмах Любовь Семеновна, доктор технических наук, ведущий научный сотрудник, ФГБУН «Институт структурной макрокинетики и проблем материаловедения им. А. Г. Мерджанова Российской академии наук (ИСМАН)», Черногловка, Российская Федерация; ORCID 0000-0003-0418-1534; e-mail: stelm@ism.ac.ru

Жидович Александра Олеговна, младший научный сотрудник, ФГБУН «Институт структурной макрокинетики и проблем материаловедения им. А. Г. Мерджанова Российской академии наук (ИСМАН)», Черногловка, Российская Федерация; ORCID 0000-0001-5083-1126; e-mail: a10012012@ism.ac.ru

Столин Александр Моисеевич, доктор физико-математических наук, профессор, заведующий лабораторией, ФГБУН «Институт структурной макрокинетики и проблем материаловедения им. А. Г. Мерджанова Российской академии наук (ИСМАН)», Черногловка, Российская Федерация; ORCID 0000-0002-5360-3388; e-mail: amstolin@ism.ac.ru

Карпов Сергей Владимирович, кандидат технических наук, доцент, кафедра «Компьютерно-интегрированные системы в машиностроении», Тамбовский государственный технический университет, Тамбов, Российская Федерация; ORCID 0000-0001-8238-1537; e-mail: karpov.sv@mail.tstu.ru

Received 17 June 2022; Accepted 29 July 2022; Published 12 October 2022



Copyright: © Stel'makh LS, Zhidovich AO, Stolin AM, Karpov SV, 2022. This article is an open access article distributed under the terms and conditions of the Creative Commons Attribution (CC BY) license (<https://creativecommons.org/licenses/by/4.0/>).